Transport in Porous Media **43:** 137–158, 2001.

Salt Water Intrusion in a Three-dimensional Groundwater System in The Netherlands: A Numerical Study

GUALBERT H.P. OUDE ESSINK
Centre of Hydrology, Department of Theoretical Geophysics, Institute of Earth Sciences, University Utrecht, 3508 TA Utrecht, The Netherlands

Abstract. Salt water intrusion is investigated in a coastal groundwater system in the northern part of the province Noord-Holland, The Netherlands. Density dependent groundwater flow is modeled in three-dimensions with MOCDENS3D. This computer code is a version of MOC3D (Konikow *et al.*, 1996) that has been adapted to simulate transient density-driven groundwater flow. Results from the model suggests that in this Dutch hydrogeologic system a severe and irreversible salinisation is already occurring. Within a few tens to hundreds of years, the salinity of the shallow aquifer is estimated to increase substantially. This salinisation process is a result of human activities such as the reclamation of the low-lying areas during the past centuries. Without changing the present boundary conditions, seepage into the low-lying areas will decrease slightly because of predicted increases in groundwater salinity. However, the rate in salt load through the Holocene aquitard into the low-lying areas will increase significantly due to an increase in salinity in the shallow aquifer. In addition, a relative sea level rise of 0.5 m per century will intensify the salinisation process, causing an enormous increase in salt load in all low-lying areas in this part of The Netherlands.

Key words: salt water intrusion, coastal aquifer, sea level rise, numerical modeling, MOCDENS3D, density-driven groundwater flow, Noord-Holland, The Netherlands.

1. Introduction

The Netherlands is a densely populated country of which some eight million people are living in the coastal zone. Due to several natural and anthropogenic causes, Dutch coastal groundwater systems are threatened by a severe intrusion of saline water. The salinisation of the groundwater systems may affect water management sectors such as agriculture, domestic and industrial water supply, and flushing of water courses of low-lying polders. A polder is an area which is protected from water outside the area and which has a controlled water level. In general, salinisation of the (sub)soil and the root zone does not occur easily under the climatic conditions in The Netherlands. Though salt accumulation is taking place in the soil in the summer, the excess of precipitation in winter flushes the salt into the water courses of the low-lying polder, and subsequently into the system of reservoirs for superfluous polder water, called a boezem. In those polders where seepage quantities and chloride loads are very high, the moisture in the root zone may contain high

salinities in summer. These high loads may cause salt damage to low salt-resistant crops. A rise in relative sea level increases the threat to the groundwater system.

The focus of this paper is the problem of salt water intrusion in one specific three-dimensional coastal groundwater system where a non-uniform density distribution occurs. The present and future distributions of fresh, brackish and saline groundwater will be discussed in the northern part of the province Noord-Holland. This area is called *De Kop van Noord-Holland*. Based on numerical results, changes in salinity, seepage and salt load are explained. In addition, the possible consequences of three scenarios of sea level rise are considered. Only a few studies have considered the effect of sea level rise on salt water intrusion in coastal aquifers, for example, the North Atlantic Coastal Plain, USA (Meisler *et al.*, 1984); the Galveston Bay, Texas, USA (Leatherman, 1984); the Potomac–Raritan–Magothy aquifer system, New Jersey, USA (Lennon *et al.*, 1986; Navoy, 1991); The Netherlands (Oude Essink, 1996; Oude Essink, 1999) and India (Bobba, 1999). In this paper, three-dimensional density-driven groundwater flow is considered, taking into account mixing of fresh and saline groundwater by means of hydrodynamic dispersion.

First, the development of the low-lying part of The Netherlands is discussed. Then the applied computer code is described. The development of the model of the considered hydrogeologic system is presented, followed by a discussion of some numerical results. Finally, conclusions are drawn and some recommendations will be made.

2. Genesis of The Netherlands: A Man-Made Environment

The major part of The Netherlands consists of lagoon and deltaic areas of the rivers Rhine, Scheldt and Meuse, created by natural processes such as rising sea levels, the forming of sand-ridges, sea invasions, and the forming of lakes in invaded land (Wesseling, 1980). Before the occupation by man, the area behind the dunes was drained by a system of broad, slowly moving streams. Flood water from the high river stages and from the sea could easily enter the area. Starting from approximately the third century BC, the inhabitants built dwelling mounds and drained flood plains to keep their feet dry. From about 1100 AD, embankments along the main rivers were constructed and sluices were built at the outlets of smaller streams to protect inhabitants and their livestock from drowning and their agricultural land from flooding. Gradually, smaller inlets were embanked resulting in a pattern of small areas surrounded by dikes, the so-called polders. Later on, the land subsided because the peaty soil was drained more efficiently. This subsidence especially occurred in peat areas of Holocene origin in the western and northern part of the country. Peat was mined in these areas for fuel, and subsequently, lakes were created. With the improvement of windmills and the paddle wheel in the sixteenth century, water from the polders could be removed more easily and it became possible to reclaim larger and deeper lakes for agriculture and development. Especially

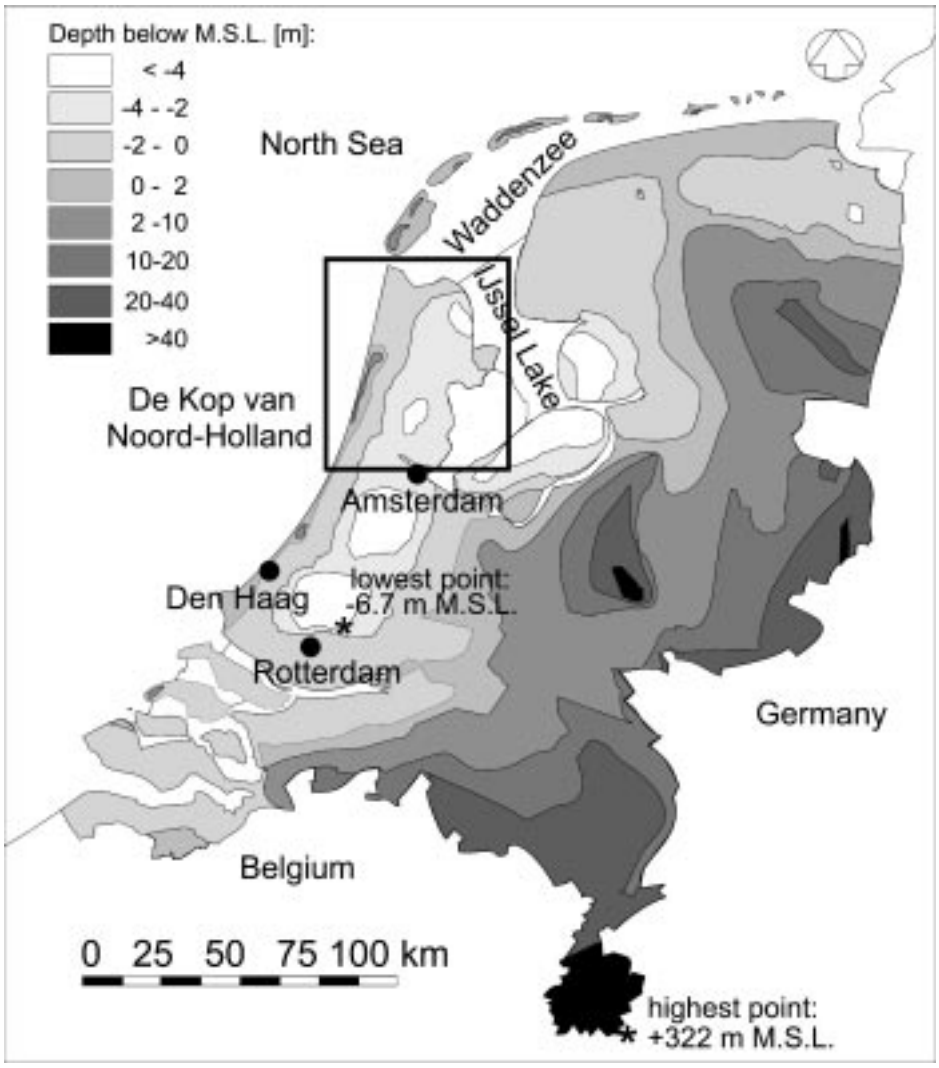

Figure 1. Present ground level in The Netherlands.

during the seventeenth century, numerous lakes were reclaimed in Noord-Holland. These so-called droogmakerijen partly originate from digging and drying peat for heating purposes. Later on, the use of steam, followed by electrical and diesel engines, lead to the reclamation of the deepest lakes (e.g. the polder Wieringermeer in 1932).

What used to be a swampy flat area with some streams and lakes is now a pattern of smaller and larger polders, each having its own embankment and a controlled phreatic water level (the so-called polder level) with a specific elevation. Figure 1 shows the present ground level of The Netherlands. About 25% of this low-lying land, especially large parts of Noord- and Zuid-Holland, is situated below mean

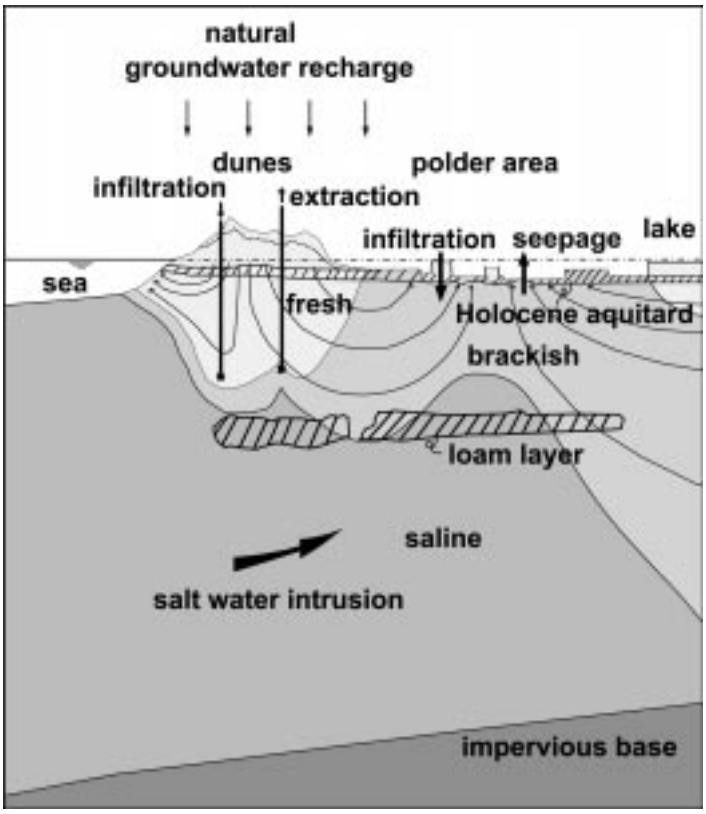

Figure 2. A schematisation of the hydrogeological situation in the coastal western part of The Netherlands.

sea level, whereas about 65% would be flooded regularly by the sea or the rivers in the absence of dunes and dikes.

The reclamation of the lakes initiated rapid changes in the groundwater system. In order to drain the polders, the controlled phreatic water level in these polders had to be lowered. Groundwater started to flow between polders because phreatic water levels in adjacent polders differed. Seepage in the polders was introduced because of the difference between the phreatic water level in the polder above the Holocene aquitard and the piezometric head in the aquifer (Figure 2). The intensity of the seepage is highly dependent on the polder geometry, the phreatic water level and hydrogeological parameters of the polders, such as the thickness and (vertical) hydraulic conductivity of aquitards. As regressions and transgressions of the sea in the western and northern part of The Netherlands had created large zones of fresh, brackish and saline groundwater in the upper parts of the groundwater system, the seepage was accompanied by a load of salt. At some polders which are surrounded by lakes, the brackish or saline seepage may eventually turn into fresh seepage (van Dam, 1976).

3. Numerical Computer Code

To simulate a groundwater system as it occurs in the area of interest, the three-dimensional computer code MOC3D (Konikow *et al.*, 1996) was adapted for density differences and is called MOCDENS3D (Oude Essink, 1998). Note that MOCDENS3D is not the three-dimensional version of the two-dimensional code MOCDENSE (Sanford and Konikow, 1985), which is based on MOC (Konikow and Bredehoeft, 1978).

As a result, it is possible to model transient groundwater flow in three-dimensional hydrogeologic systems where non-uniform density distributions occur. Special fields of application of MOCDENS3D are heat transport in porous media and salt water intrusion in coastal aquifers, a topic which is extensively described in Bear *et al.* (1999).

The groundwater flow equation is solved by the so-called MODFLOW module of MOCDENS3D, which is basically the MODFLOW computer code (McDonald and Harbaugh, 1988; Harbaugh and McDonald, 1996). The freshwater head ϕ_f, which is introduced to take into account differences in density in the calculation of the head, is defined as:

$$\phi_f = \frac{p}{\rho_f g} + z, \tag{1}$$

where ϕ_f is the freshwater head $[L]$, p is the pressure $[ML^{-1}T^{-2}]$, ρ_f is the reference density, usually the density of fresh groundwater (without dissolved solids) at mean subsoil temperature, g is the gravity acceleration $[LT^{-2}]$, and z is the elevation head $[L]$. The vertical Darcian velocity (specific discharge) is defined as follows:

$$q_z = -\frac{\kappa_z}{\mu}\left(\frac{\partial p}{\partial z} + \rho g\right), \tag{2}$$

where κ_z is the vertical intrinsic permeability $[L^2]$ and μ is the dynamic viscosity $[ML^{-1}T^{-1}]$. Combination of the Equations (1) and (2) gives:

$$q_z = -\frac{\kappa_z \rho_f g}{\mu}\left(\frac{\partial \phi_f}{\partial z} + \frac{\rho - \rho_f}{\rho_f}\right). \tag{3}$$

Viscosity differences may be neglected if density differences are small (Verruijt, 1980, Bear and Verruijt, 1987). As such, Equation (3) can be written as

$$q_z = -k_z\left(\frac{\partial \phi_f}{\partial z} + \frac{\rho - \rho_f}{\rho_f}\right), \tag{4}$$

where $k_z = \kappa_z \rho_f g/\mu$ is the hydraulic conductivity for fresh water and $(\rho - \rho_f)/\rho_f$ is the buoyancy term. Note that in cases with high groundwater densities, such as brine transport in salt domes with densities over 1200 kg/m^3, Equation (3) instead of Equation (4) should be used.

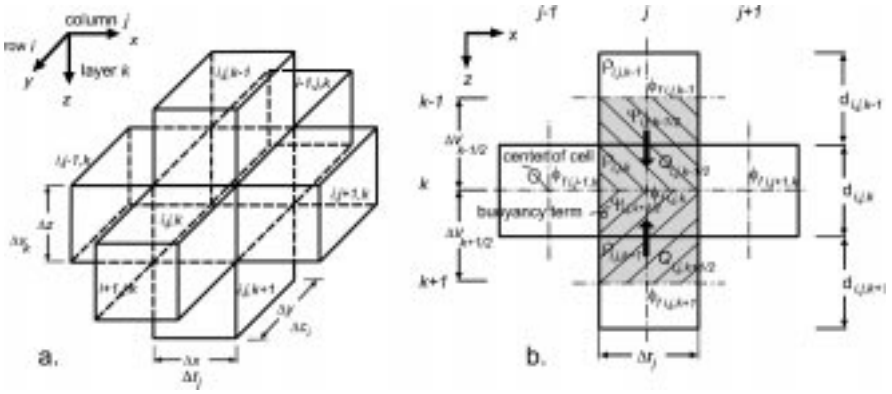

Figure 3. MODFLOW cells with corresponding density terms.

Discretisation of the buoyancy term, which is a new term in the MODFLOW module, gives (Figure 3)

$$\Psi_{i,j,k+1/2} = \frac{(\rho_{i,j,k} + \rho_{i,j,k+1})/2 - \rho_{\mathrm{f}}}{\rho_{\mathrm{f}}}, \tag{5}$$

where $\Psi_{i,j,k+1/2}$ is the discretised buoyancy term of the cells $[i, j, k]$ and $[i, j, k+1]$. Equation 4 is then rewritten in discretised terms as used in the MODFLOW module (note that the z-axis is pointing vertically downward, as used in MODFLOW). In combination with Equation (5), the flow at the top of cell $[i, j, k]$ is

$$q_{i,j,k-1/2} = +KV_{i,j,k-1/2}\left(\frac{\phi_{\mathrm{f},i,j,k-1} - \phi_{\mathrm{f},i,j,k}}{\Delta v_{k-1/2}} + \Psi_{i,j,k-1/2}\right), \tag{6}$$

where $KV_{i,j,k-1/2}$ is the discretised hydraulic conductivity between the cells $[i, j, k-1]$ and $[i, j, k]$ $[L^2T^{-1}]$, and $\Delta v_{k-1/2}$ is the distance between the cells $[i, j, k-1]$ and $[i, j, k]$ $[L]$. Similar for the flow at the bottom of cell $[i, j, k]$

$$q_{i,j,k+1/2} = -KV_{i,j,k+1/2}\left(\frac{\phi_{\mathrm{f},i,j,k} - \phi_{\mathrm{f},i,j,k+1}}{\Delta v_{k+1/2}} + \Psi_{i,j,k+1/2}\right). \tag{7}$$

The vertical Darcian velocity q is multiplied by the area $\Delta r_j\ \Delta c_i$ to derive the volume flow Q. By using the so-called conductance in the vertical direction, $CV_{i,j,k-1/2} = KV_{i,j,k-1/2}\,\Delta r_j \Delta c_i / \Delta v_{k-1/2}$ (McDonald and Harbaugh, 1988), Equation (6) is written as

$$Q_{i,j,k-1/2} = CV_{i,j,k-1/2}(\phi_{\mathrm{f},i,j,k-1} - \phi_{\mathrm{f},i,j,k} + \Psi_{i,j,k-1/2}\Delta v_{k-1/2}) \tag{8}$$

and similar for Equation (7)

$$Q_{i,j,k+1/2} = CV_{i,j,k+1/2}(\phi_{\mathrm{f},i,j,k+1} - \phi_{\mathrm{f},i,j,k} - \Psi_{i,j,k+1/2}\Delta v_{k+1/2}). \tag{9}$$

The thicknesses d of all cells in the grid are known values in the solute transport module of MOCDENS3D. As such, $\Delta v_{k-1/2}$ and $\Delta v_{k+1/2}$ can be rewritten as $(d_{i,j,k-1} + d_{i,j,k})/2$ and $(d_{i,j,k} + d_{i,j,k+1})/2$, respectively (Figure 3).

Density differences are taken into account through adding the two buoyancy terms of the Equations (8) and (9) to the right-hand side term (RHS term) of the basic groundwater flow equation of MODFLOW (McDonald and Harbaugh, 1988)

$$RHS^{\text{new}}_{i,j,k} \quad \text{becomes} \quad RHS^{\text{old}}_{i,j,k} - CV_{i,j,k-1/2}\Psi_{i,j,k-1/2}(d_{i,j,k-1} + d_{i,j,k})/2 + \\ + CV_{i,j,k+1/2}\Psi_{i,j,k+1/2}(d_{i,j,k} + d_{i,j,k+1})/2. \tag{10}$$

Similar adaptations were implemented by Lebbe (1983) and Sanford and Konikow (1985) for the two-dimensional solute transport code MOC (Konikow nd Bredehoeft, 1978). Because density variations in the considered system remain small in comparison with the reference density ρ_{f}, changes in density are mathematically neglected in the continuity equation of MOCDENS3D except from the buoyancy term ρg in Darcy's law (Holzbecher, 1998). As such, the Oberbeck–Boussinesq approximation is applicable.

The velocities, adapted for density differences by introducing the buoyancy terms, are derived from the freshwater head distribution. Subsequently, the velocity field is used in the solute transport module to simulate changes in the concentration distribution, and thus, the density distribution. As such, the groundwater flow and solute transport modules are coupled with each other.

An advantage of applying the method of characteristics for solving the advection-dispersion equation is that the restrictions on spatial discretisation (characterized by the grid Peclet number) are not strict. This is in contrast with codes that solve the advection-dispersion equation by the standard finite-difference and finite-element methods (Jensen and Finlayson, 1978; Frind and Pinder, 1983; Daus *et al.*, 1985; Kinzelbach, 1987; Oude Essink and Boekelman, 1996). As a consequence, the displacement of fresh, brackish and saline groundwater in large-scale groundwater systems can be modeled easily without numerical problems such as an excess of numerical dispersion, large numerical oscillations or non-convergence of the solute transport equation.

A linear equation of state couples groundwater flow and solute transport

$$\rho(C) = \rho_{\text{f}}[1 + \beta_C(C - C_0)], \tag{11}$$

where $\rho(C)$ is the density of groundwater $[ML^{-3}]$, C is the chloride concentration $[ML^{-3}]$, β_C is the volumetric concentration expansion gradient $[L^3M^{-1}]$, and C_0 is the reference chloride concentration $[ML^{-3}]$.

MOCDENS3D takes into account hydrodynamic dispersion (molecular diffusion and mechanical dispersion), expressed through the conventional notation

$$D_{ij} = (D_m + \alpha_{\text{T}}|V|)\delta_{ij} + (\alpha_{\text{L}} - \alpha_{\text{T}})\frac{V_i V_j}{|V|}, \tag{12}$$

where D_{ij} is the coefficient of hydrodynamic dispersion $[L^2T^{-1}]$, D_m is the coefficient of molecular diffusion $[L^2T^{-1}]$, α_{L} is the longitudinal dispersivity of the

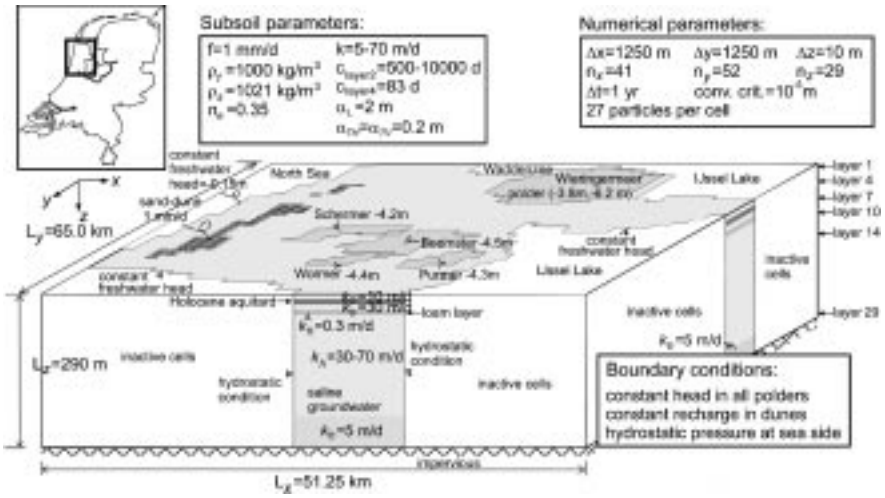

Figure 4. The geometry of the groundwater system in *De Kop van Noord-Holland*.

aquifer $[L]$, α_T is the transversal dispersivity of the aquifer $[L]$, V_i and V_j are the components of the effective velocity in the i and j directions respectively $[LT^{-1}]$, $|V|$ is the magnitude of the effective velocity $[LT^{-1}]$, and $\delta_{ij} = 1$ if $i = j$ and $\delta_{ij} = 0$ if $i \neq j$. The advection-dispersion equation is solved by the method of characteristics. See Konikow and Bredehoeft (1978) and Konikow *et al.* (1996) for a detailed description of the applied numerical techniques.

4. Model Development and Calibration

4.1. MODEL DEVELOPMENT

The groundwater system of interest is approximately $65.00 \times 51.25\,\text{km}^2$ (see Figure 4), and is covered with a 3D grid. The sizes of each cell are $\Delta x = 1250\,\text{m}$, $\Delta y = 1250\,\text{m}$ and $\Delta z = 10\,\text{m}$. The grid contains 61828 cells: $n_x = 41$, $n_y = 52$, $n_z = 29$, where n_i denotes the number of cells in the i direction. Due to the rugged coastline of the groundwater system, only 64.6% of the cells (39933 out of 61828) are considered as active cells. Each cell contains 27 particles to solve the advection term of the solute transport equation. As such, 1078191 particles are used initially. The flow time step Δt to recalculate the groundwater flow equation equals one year.

The data for model development are obtained from various sources such as the Institute for Land and Water Management Research (1982); TNO (1979); Beekman (1991); Paap (1992) and TNO-GG/RIZA (1994). These reports give detailed information about hydrogeological data of the area of interest, such as solute concentrations (including some time series of chloride concentration), piezometric heads at various depths, water and solute balance figures, and subsoil parameters (hydraulic conductivities and positions of aquifers and aquitards).

The groundwater system consists of good permeable aquifers of Quaternary deposits, intersected by a loamy aquitard and overlain by a Holocene aquitard of clayey and peat composite. As such, the hydraulic conductivity varies in the system: in the top layer $k_x = 10$ m/d; the second layer consists of an aquitard with hydraulic resistances varying from 500 days to 10000 days. The hydraulic resistance c $[T]$ is the reciprocal value of the leakage coefficient γ $[T^{-1}]$, and equals the thickness of the aquitard divided by its vertical hydraulic conductivity. The fourth layer consists of an aquitard with a hydraulic resistance equal to 83 days ($k_x = 0.3$ m/d). For layers 3 and 5 $k_x = 30$ m/d, for layer 6 $k_x = 40$ m/d, for layers 7 to 10 $k_x = 50$ m/d and for layers 11 to 22 $k_x = 70$ m/d. From layer 23 down to layer 29 $k_x = 70$ m/d, but deposits of the formation of Maassluis, which have a relatively low hydraulic conductivity of 5 m/d, are also included at these depths. An impermeable hydrogeologic base is assumed at -290 m N.A.P. (Normaal Amsterdams Peil, N.A.P., roughly equals Mean Sea Level and is the reference level in The Netherlands), as the layers below have very low permeabilities. The anisotropy ratio k_z/k_x equals 0.4 for all layers. The effective porosity n_e is 0.35. The longitudinal dispersivity α_L is equal to 2 m, while the ratio of transversal to longitudinal dispersivity α_T/α_L is 0.1. For a conservative solute as chloride, the molecular diffusion D_m for porous media is taken equal to 10^{-9} m^2/s. The specific storativity S_s $[L^{-1}]$ can be set to zero on the applied time scale.

Hydrostatic conditions occur at the four sides. At the top of the system, the water level at the sea is -0.15 m N.A.P. and constant in time in the case of no sea level variation. The IJssel Lake, which is maximum 10 m deep, used to have an open connection with the sea. In 1932, an enclosure dam was constructed and the inland sea rapidly became a freshwater lake. In winter the water level strived after is -0.4 m N.A.P. and in summer -0.2 m N.A.P. A large number of low-lying polders is present in the system with an area of approximately 2000 km^2. The phreatic water level in the polders differs for each polder, varying from -0.1 m to -6.2 m N.A.P., and is kept constant in time, see Figure 5. As such, relatively small seasonal fluctuations in the phreatic water level (polder level) are neglected.

At the initial situation (1990 AD), the hydrogeologic system contains saline, brackish as well as fresh groundwater. Figure 6 gives the estimated chloride concentration in six layers. Some 3000 chloride analyses in 900 observation wells, summarized in a report of the Institute for Land and Water Management Research (1982), were used to guide the development of the initial chloride distribution. The salinity increases with depth, with freshwater lenses at the sand-dune areas and a freshwater reservoir under the city of Hoorn. The volumetric concentration expansion gradient β_C is 1.34×10^{-6} l/mg Cl$^-$. Saline groundwater in the lower layers does not exceed 16000 mg Cl$^-$/l, as sea water that intruded the groundwater system has been mixed with water from the river Rhine. The corresponding density ρ of that saline groundwater equals about 1021.5 kg/m^3.

In the sand-dune area, the constant natural groundwater recharge equals 1 mm/d. Groundwater is extracted from the sand-dune areas at -25 m N.A.P. with an amount

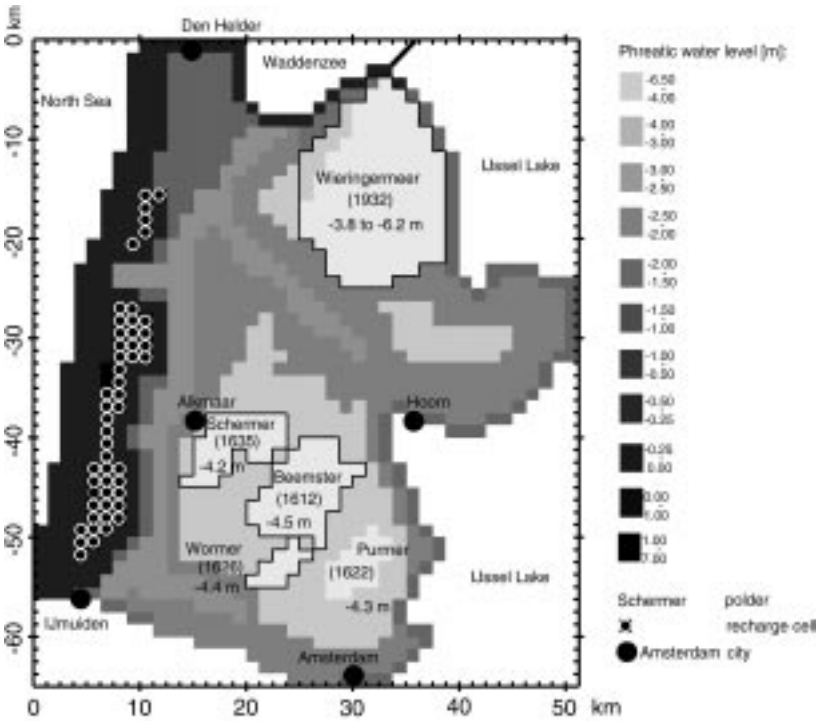

Figure 5. Present phreatic water level in the top layer (1990 AD). Between brackets the date of reclamation of the polder. The following five polders have a very low phreatic water level: Wieringermeer, Schermer, Beemster, Wormer, and Purmer. The recharge in the sand-dune area is equal to 1 mm/d.

of 5.2 million m^3/yr and from wells distributed over the eastern and southern part of the polder area at -35 m N.A.P. with a total amount of 5.4 million m^3/yr. Large industrial withdrawals are pumped from the southwestern corner of the model (22.5 million m^3/yr between -115 and -135 m N.A.P.).

4.2. CALIBRATION

The calibration run is executed with MOCDENS3D based on the input data discussed in the previous subsection. The Strongly Implicit Procedure needs about three hundred fifty iterations to meet the convergence criterion of 10^{-5} m for the groundwater flow equation (freshwater head). The groundwater system is calibrated for 1990 AD conditions with freshwater head distributions at different elevations, with seepage and salt load quantities through the top aquitard in five polders (viz. Wieringermeer, Schermer, Beemster, Wormer and Purmer), with recharge figures in the sand-dune areas. Anisotropy, hydraulic conductivities, hydraulic resistances, phreatic water levels, boundary conditions, but especially the initial chloride distribution are changed to improve the fit between simulation results

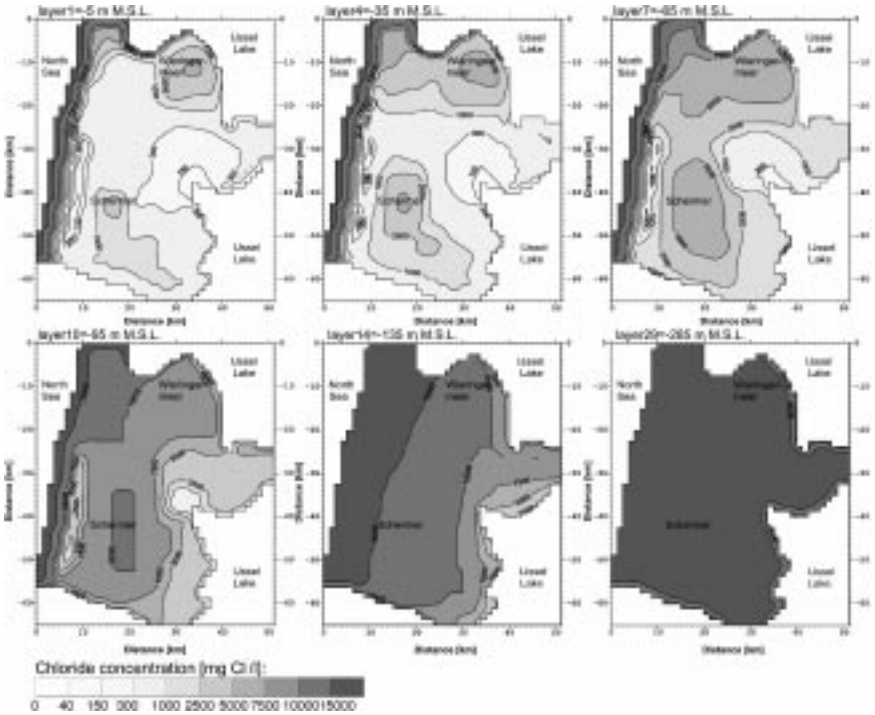

Figure 6. Initial chloride concentration in the hydrogeologic system at the beginning of the simulation (1990 AD) at six layers: −5 m, −35 m, −65 m, −95 m, −135 m and −285 m N.A.P.

and measurements. Major adjustments of these subsoil parameters were needed to satisfactorily calibrate the system. For instance, the initial computed salt load values in the polders correspond with measured ones (Institute for Land and Water Management Research, 1982).

Note that it is strictly not valid to calibrate this model with only one ‘snapshot’ in time, viz. 1990 AD, because the model will be used to simulate the transient process of salt water intrusion. The problem is that only a few observations of chloride concentration as a function of some several tens of years are available to calibrate the transient model. This limitation will to some point negatively effect the reliability of the numerical results.

Figure 7 shows the computed freshwater head distribution in four layers 3, 7, 13 and 29 at 1990. The low-lying polders cause a low freshwater head in the center of the hydrogeologic system, inducing an inflow of brackish and saline groundwater from the sea and the IJssel Lake. Seepage especially occurs in the low-lying polder areas (Figure 8(a)). The computed total seepage quantity out of the system at 1990 equals 144 million m^3 per year, which compares well to measured values (Institute for Land and Water Management Research, 1982). In the northeastern part of the polder Wieringermeer, the seepage quantity can be as high as 5.6 mm/d, which is mainly caused by the low hydraulic resistance of the Holocene aquitard in that area.

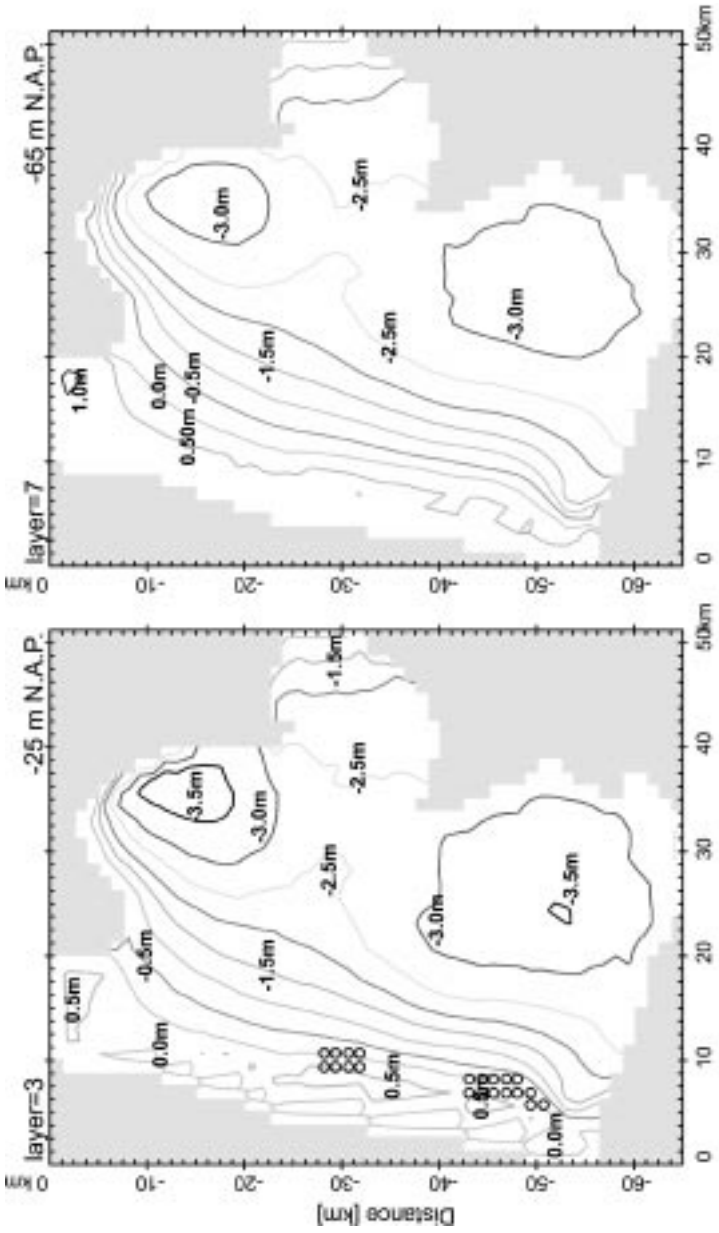

Figure 7. Computed freshwater head at four layers: −25 m, −65 m, −125 m and −285 m N.A.P.

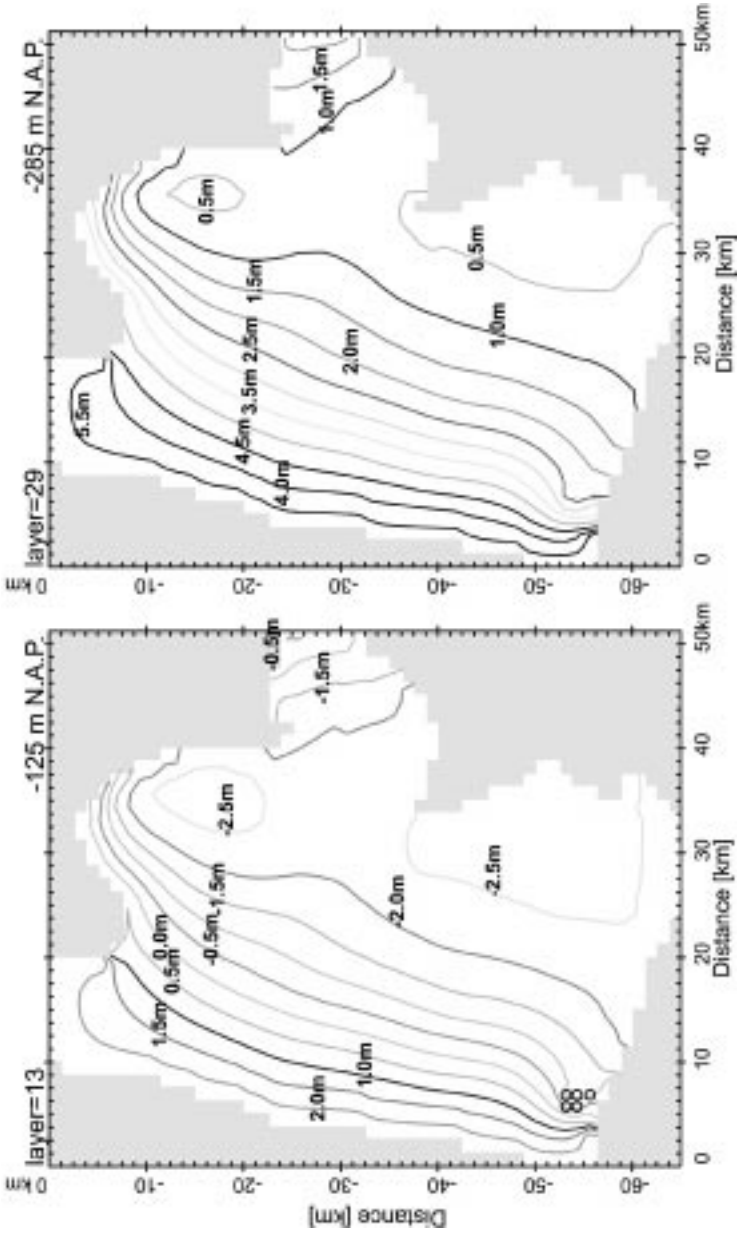

Figure 7. continued

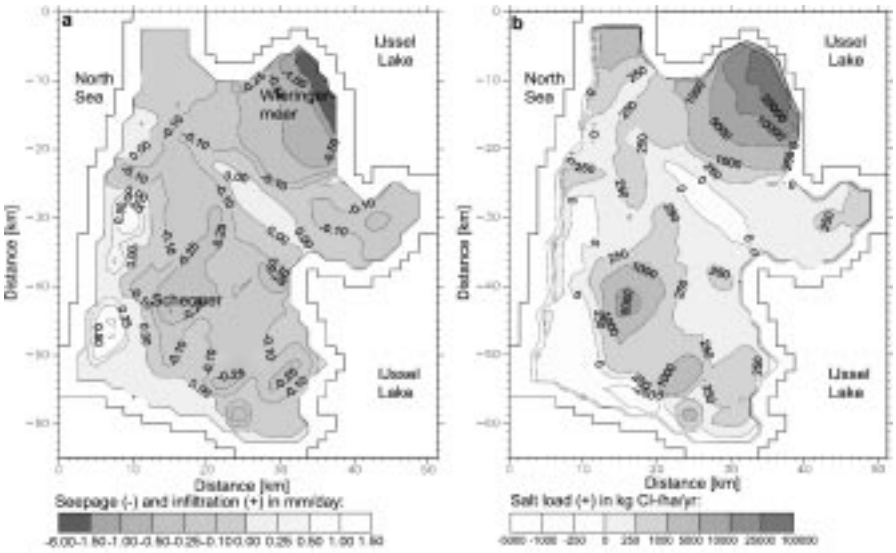

Figure 8. Seepage in mm/day (a) and salt load in kg Cl^-/ha/yr (b) at 1990 AD through the top aquitard at -20 m N.A.P.

Figure 8(b) shows the salt load in the hydrogeologic system through the bottom of the top aquitard at -20 m N.A.P. The initial chloride concentration distribution, which partly determines the salt load, had to be adjusted several times to improve calibration. The total computed and measured values of salt load also compare well: computed 400×10^3 ton Cl^- per year versus measured 457×10^3 ton Cl^- per year (Institute for Land and Water Management Research, 1982), of which at least 80% comes from the polder Wieringermeer.

In addition, the effect of the longitudinal dispersivity α_L on the salinity distribution is investigated. In contrast with some other field sites (e.g., see the cases in Gelhar *et al.* (1992)), the best estimates of the longitudinal dispersivities in Dutch and Belgian large-scale aquifer systems with Holocene and Pleistocene deposits of marine and fluviatile origin appear to yield rather small values. This observation is based on various case studies, such as Lebbe (1983), Kooiman (1989) and Stuyfzand (1993). Nevertheless, the sensitivity of the model to longitudinal dispersivities is briefly evaluated. For this purpose, the calibrated situation of 1990 AD is simulated for 1000 years with four different longitudinal dispersivities, viz. α_L is 2 m (this case is called the reference case), and for α_L is 0 m, 10 m and 50 m. When comparing the numerical results of the two cases with $\alpha_L = 2$ m and $\alpha_L = 0$ m, the chloride distribution is slightly different though the brackish zones become somewhat smaller if $\alpha_L = 0$ m. It appears that the two values $\alpha_L = 10$ m and $\alpha_L = 50$ m are probably too large, as the freshwater lenses at the sand-dune areas (Cl^- concentration < 150 mg Cl^-/l) disappear over time, which is very unlikely in this geometry if the sea level would stay constant. In addition, groundwater in

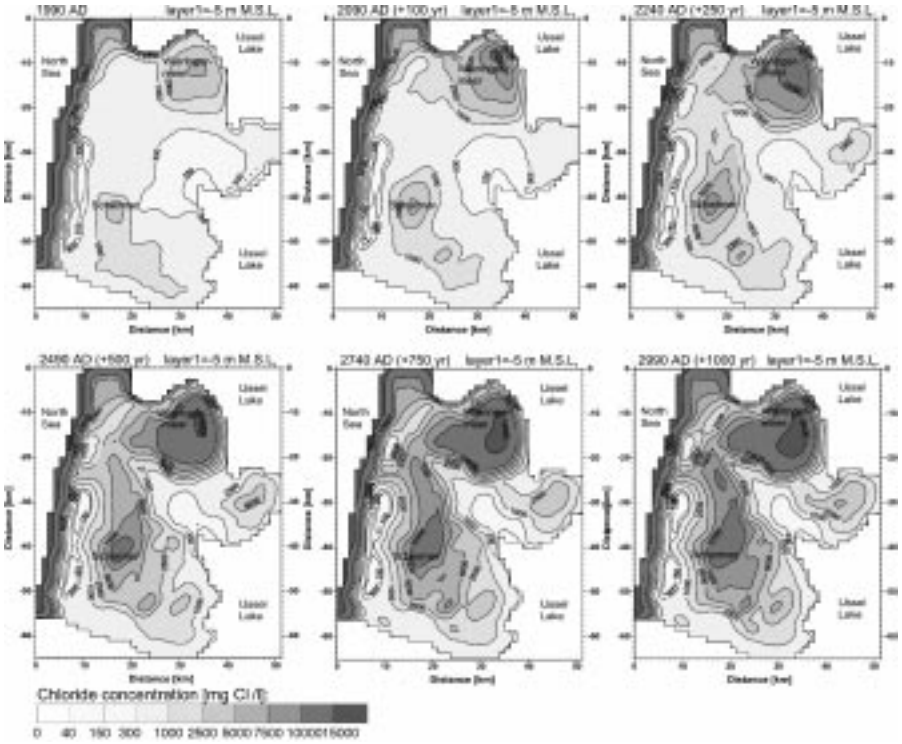

Figure 9. Computed chloride concentration in the top layer at −5 m N.A.P. in the hydrogeologic system at six moments in time: 1990, 2090, 2240, 2490, 2740 and 2990 AD. An enormous increase in salinity is detected in the polders Wieringermeer and Schermer.

the lower layers becomes less saline due to an excessive mixing process. This is also unlikely, as a strong inflow of saline groundwater would certainly increase the salinity in the lower part of the hydrogeologic system.

5. Discussion

5.1. SALT WATER INTRUSION: NO SEA LEVEL RISE

The reference case, which is the case with α_L is 2 m (see the previous subsection Calibration), is discussed here in detail. Note that the boundary conditions, such as the level of the North Sea, are kept constant during the time period of 1000 years. Figure 9 shows the computed chloride concentration in the top layer of the hydrogeologic system at −5 m N.A.P. at six moments in time: 1990 AD (the initial situation), 2090 AD, 2240 AD, 2490 AD, 2740 AD and 2990 AD. As can be seen, the chloride concentration increases significantly, especially in the low-lying polders Wieringermeer and Schermer. The salinity in the total hydrogeologic system increases, especially in the coming centuries (Figure 10). Saline groundwater intrudes into the system because it is attracted by the polders which have low

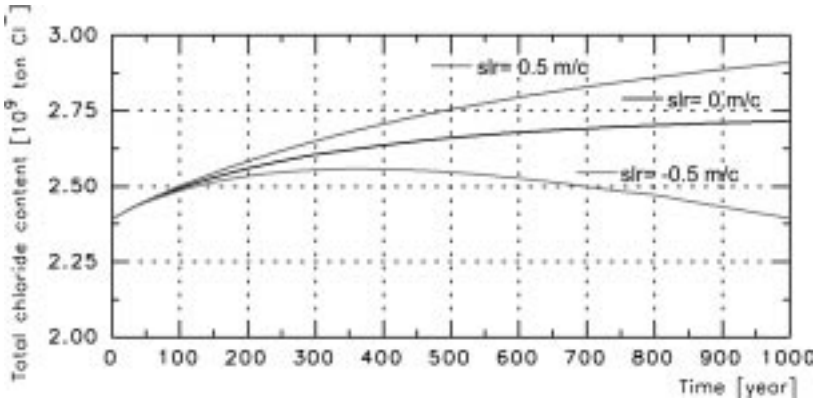

Figure 10. Total chloride (in 10^9 ton Cl^-) in the entire hydrogeologic system as a function of time: 'slr' stands for sea level rise.

phreatic water levels. Salt water intrusion seriously started at the moment the low-lying polders Schermer, Beemster, Wormer and Purmer were reclaimed during the beginning of the seventeenth century.

The model suggests that saline groundwater enters the system with an average velocity in the order of 10 m per year. This implies that the system has not reached steady state. For instance, it appears that saline groundwater, which currently enters the groundwater system from the North Sea will take nearly thousand years to reach the first low-lying polder Schermer, 10 km from the coast. This conclusion is deduced from a straightforward calculation using streamlines based on the present velocity field in a vertical plane. As the Schermer was reclaimed in 1635, sea water has already intruded the system for some 365 years. Based on the present velocity field, this sea water will need an additional six and a half centuries to reach the aquifer beneath the Schermer.

5.2. EFFECT OF SEA LEVEL RISE

The effect of a variation in sea water level is investigated next. According to the Intergovernmental Panel of Climate Change Second Assessment Report (Warrick *et al.*, 1996), a sea level rise of 0.49 m is to be expected for the year 2100, with an uncertainty range from 0.20 to 0.86 m. This rate is two to five times the rate experienced over the last century. In this paper, three scenarios of sea level variation are considered for the coming millennium: a sea level rise of 0.5 m per century, no sea level rise (which is the reference case) and a sea level rise of -0.5 m per century (thus a sea level fall). Land subsidence, which is caused by groundwater recovery, compaction and shrinkage of clay, and oxidation of peat also contributes to the relative rise in sea level. It is likely that, besides the change in sea level, some other boundary conditions will vary during the course of the coming 1000 years. For example, the position of the coastline may not be fixed in the course

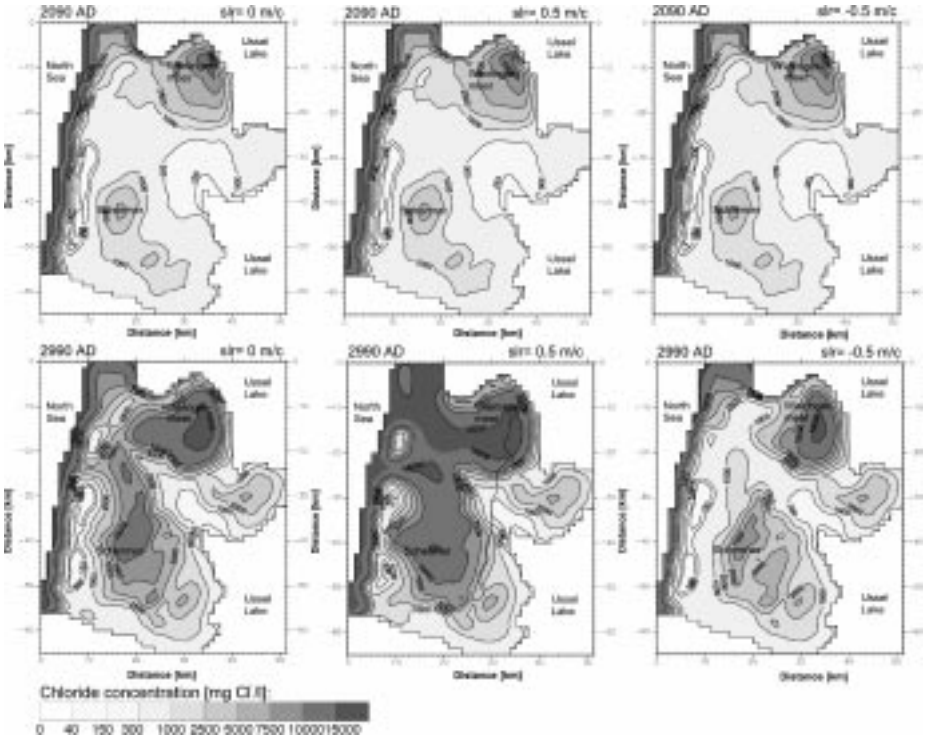

Figure 11. Chloride concentration in the top layer at −5 m N.A.P. in the hydrogeologic system for three sea level rise (slr) scenarios (0 m/c, 0.5 m/c and −0.5 m/c) at two moments in time: 2090 and 2990 AD.

of the simulation time of 1000 years, especially in case of a sea level change. In addition, the level of the IJsselmeer will probably be adapted to the changing sea level. However, for reasons of simplicity, changes in these and other boundary conditions of the surface water system are not taken into account in this study. Figure 11 shows the computed chloride concentration in the top layer at −5 m N.A.P. for all three sea level rise scenarios at two moments in time: 100 years and 1000 years after the initial situation at 1990 AD (thus at 2090 AD and at 2990 AD). During the coming centuries, the salinity in the groundwater system increases in all three cases, compared to the initial situation (see also Figure 10). Obviously, the most serious increase in salinity is obtained when the sea level rises 0.5 m/c. However, the low-lying polders will also experience saline groundwater in the top layer in case of no sea level rise and even in case of a sea level rise of −0.5 m/c.

5.3. EFFECTS ON FIVE SELECTED POLDERS

Consider the five selected polders Wieringermeer, Schermer, Beemster, Wormer and Purmer (see Figure 5 for the exact position in the system). Figure 12 shows the change in seepage in the five polders as well as the entire groundwater system for

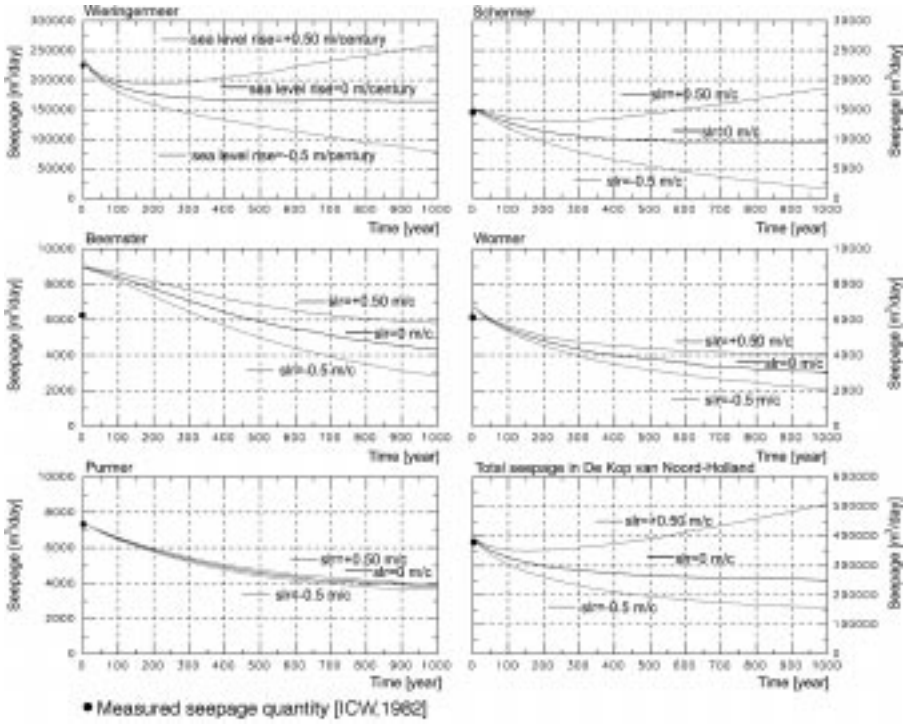

Figure 12. Seepage (in m^3/day) as a function of time for three sea level rise scenarios (0 m/c, 0.5 m/c and −0.5 m/c) in the five selected polders Wieringermeer, Schermer, Beemster, Wormer and Purmer, as well as the total seepage in *De Kop van Noord-Holland.*

all three sea level rise scenarios. The present seepage quantity, determined through the bottom of the Holocene aquitard at −20 m N.A.P., is enormous in the polder Wieringermeer due to its short distance to the lake IJsselmeer with its high lake level, but especially due to the low hydraulic resistance of the aquitard (500–4000 days). At first sight, it is remarkable that seepage quantities in all polders start to decrease significantly, compared with the initial situation. This is because of the increase in salinity in the hydrogeologic system. As salinity increases, upward flow gradients in the system decrease. As a result, the freshwater head, which takes density differences into account, is adjusted to lower values. Whereas the phreatic water levels in the polders remain the same, the seepage quantity decreases accordingly. On the other hand, the salt load, which is the product of seepage and salinity, increases substantially as the salinity in the upper layers increases.

Figure 13 shows an increase in salt load in all five polders as well as the entire groundwater system at the bottom of the Holocene aquitard at −20 m N.A.P. In all five polders the salt load increases substantially, even in case of a sea level rise of −0.5 m/c. If sea level rise is zero, the salt load has not reached a steady state situation in the first centuries of the simulation.

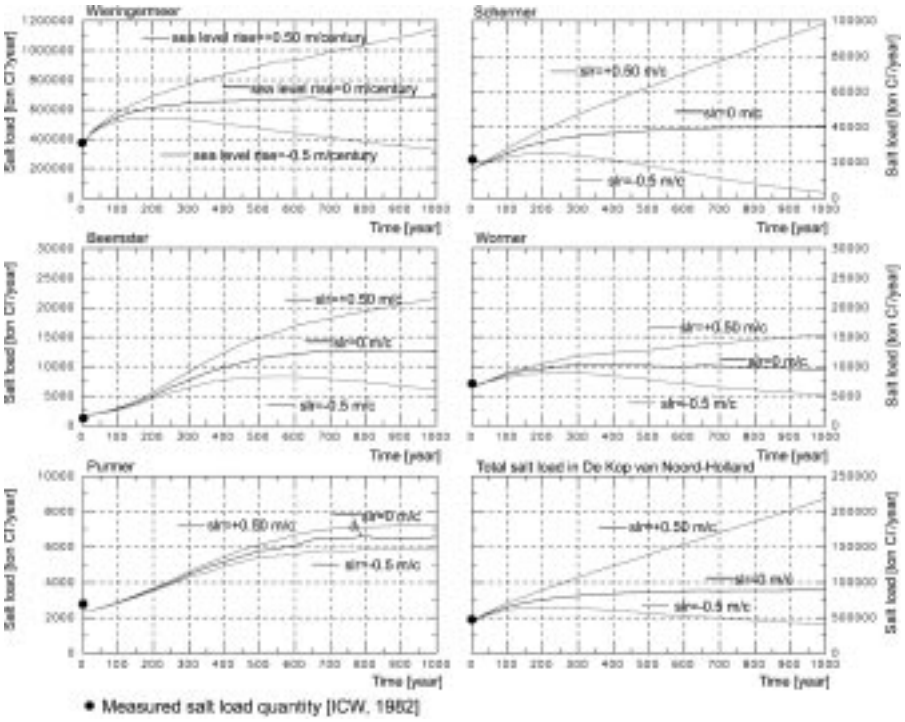

Figure 13. Salt load (in ton Cl^- per year) as a function of time for three sea level rise scenarios (0 m/c, 0.5 m/c and -0.5 m/c) in the five selected polders Wieringermeer, Schermer, Beemster, Wormer and Purmer, as well as the total salt load in *De Kop van Noord-Holland*.

The effect of a sea level variation is noticeable only after at least one century. It depends, among other factors, on the distance of the polder under consideration to the coast, how fast the effect of a sea level variation is noticeable. For instance, the Purmer is situated at a large distance from the sea. As such, the difference in salt load due to sea level rise is small. On the other hand, the salinity as well as the salt load in the Schermer increases enormously when sea level rises because the polder is lying in the zone of influence of sea level rise. Even if the sea level falls, the salinity first increases for two centuries before it slowly decreases. This phenomenon is caused by brackish and saline groundwater which is already present in the hydrogeologic system underneath the Schermer and is about to flow out of the system as seepage. After some centuries the level of the sea becomes lower than the fixed phreatic water level in some polders, and surface water starts to infiltrate there. Note that for the other polders closer to the lake IJsselmeer, the assumed constant water level in this lake dominates the flowing process through the Holocene aquitard into the polders nearby.

Note that the strong increase in salt load at the beginning of the simulation may partly be explained by a conceptual error: the effect of the estimated initial chloride distribution. If the initial chloride concentrations in the layers below -20 m N.A.P.

are taken too high in the numerical model, the computed salt load in areas with seepage will increase too strongly compared to reality. On the other hand, there is a strong indication that the salt load will increase strongly due to a physical reason, as saline groundwater already present in the lower part of the groundwater system, is about to enter the upper part of the system.

6. Conclusions

The computer code MOCDENS3D can be applied to simulate density-driven groundwater flow in a large-scale three-dimensional hydrogeologic system without numerical problems. Longitudinal dispersivities should be kept to low values, to assure that freshwater lenses remain and salt water intrudes the system. Changes in salinity are estimated over a period of 1000 years. A severe salt water intrusion is taking place in the groundwater system due to low phreatic water levels in the entire polder area. Seepage quantities in the five selected polders continue to decrease due to a decrease in upward flow gradients in the hydrogeologic system, caused by an increase in salinity. Salt load quantities increase enormously due to the salinisation of the hydrogeologic system. Sea level variations have a significant influence on the salinisation process though this is with a considerable time lag. It takes some centuries before the effect of a sea level rise of 0.5 m/c is noticed in the polders lying kilometers from the coastline. However, a sea level rise of 0.5 m/c will significantly increase the salinity in low-lying polders relatively close to the sea, such as the polders Schermer and Wieringermeer.

7. Recommendations

Obviously, initial subsoil and boundary conditions highly determine the numerical modeling of salt water intrusion in the hydrogeologic system. For instance, the hydraulic resistance of the Holocene top aquitard as well as the longitudinal dispersivity significantly effect the modeling of the salinisation process. Especially with the modeling of density-dependent groundwater, the initial density distribution should be known accurately. Unfortunately, large amounts of reliable data are not available, and more measurements should be taken. The collection and the analysis of reliable groundwater data should be intensified, varying from subsoil parameters to records of solute concentrations and piezometric heads as functions of time and space. The salinisation of the subsoil, the seepage quantities and the chloride loads in the polder areas should be monitored as functions of time to detect long term changes and to improve calibration of the transient model.

In addition, a model should be constructed which begins before the reclamation of the low-lying areas and should continue through 1990–2990. By this approach, the problem of estimating the initial chloride distribution would be eliminated and dispersivities might be calibrated in a better way.

Acknowledgements

The author highly appreciated the useful suggestions to improve the manuscript of Mark Bakker of the University of Nebraska. Reinder Boekelman of the Delft University of Technology and Toon Leijnse of the Netherlands National Institute of Public Health and Environmental Protection are thanked for the fruitful discussions throughout the course of this work. Finally, the reviewers are thanked for their detailed suggestions to improve the paper.

References

Bear, J. and Verruijt, A.: 1987, *Modeling Groundwater Flow and Pollution*, D. Reidel Publishing Company, Dordrecht, The Netherlands, 414 pp.

Bear, J., Cheng, A., Sorek, S., Herrera, I. and Ouazar, D. (eds): 1999, *Seawater Intrusion in Coastal Aquifers; Concept, Methods and Practices*, Kluwer Academic Publishers, 625 pp.

Beekman, H. E.: 1991, *Ion chromatography of fresh- and seawater intrusion, multicomponent dispersive and diffusive transport in groundwater*. PhD Thesis, Free University of Amsterdam, The Netherlands.

Bobba, A.G.: 1999, Application of a numerical model to predict freshwater depth in islands due to climate change: Agatti Island, India, *J. Environ. Hydr.* **6**.

Harbaugh, A. W. and McDonald, M. G.: 1996, User's documentation for the U.S. Geological Survey modular finite-difference ground-water flow model, *U.S. Geol. Surv. Open-File Rep. 96–485*, 56 pp.

Holzbecher, E.: 1998, *Modeling Density-Driven Flow in Porous Media, Principles, Numerics, Software, Springer Verlag, Berlin Heidelberg*, 286 pp.

Daus, A. D., Frind, E. O. and Sudicky, E. A.: 1985, Comparative error analysis in finite element formulations of the advection-dispersion equation, *Adv. Water Resour.* **8**, 86–95.

Frind, E. O. and Pinder, G. F.: 1983, The principle direction technique for solution of the advection-dispersion equation, *Proc. 10th IMACS World Congress on Systems Simulation and Scientific Computation*, Concordia University, Montreal, Canada, Aug. 1982, pp. 305–313.

Gelhar, L. W., Welty, C. and Rehfeldt, K. R.: 1992, A critical review of data on field-scale dispersion in aquifers, *Water Resour. Res.* **28**, 1955–1974.

ICW, Institute for Land and Water Management Research: 1982, Kwantiteit en kwaliteit van grond- en oppervlaktewater in Noord-Holland benoorden het IJ, (in Dutch), *Werkgroep Noord-Holland, ICW Regionale Studies 16, Wageningen*, 166 pp.

Jensen, O. K. and Finlayson, B. A.: 1978, Solution of the convection-diffusion equation using a moving coordinate system, *Second Int. Conf. on Finite Elements in Water Resoures*, Imperial College, London, pp. 4.21–4.32.

Kinzelbach, W. K. H.: 1987, *Numerische Methoden zur Modellierung des Transport von Schadstoffen im Grundwasser*, (in German), Schriftenreihe GWF Wasser-Abwasser, Band 21, R. Oldenbourg Verlag GmbH, Munchen, 343 pp.

Konikow, L. F. and Bredehoeft, J. D.: 1978, Computer model of two-dimensional solute transport and dispersion in ground water, U.S. Geol. Surv. Techn. of Water-Resour. Invest., Book 7, Chapter C2, 90 pp.

Konikow, L. F., Goode, D. J. and Hornberger, G. Z.: 1996, A three-dimensional method-of-characteristics solute-transport model (MOC3D), U.S. Geol. Surv. Water-Res. Invest. Rep. 96-4267, 87 pp.

Kooiman, J. W.: 1989, Modelling the salt-water intrusion in the dune water-catchment area of the Amsterdam Waterworks, *Proc. 10th Salt Water Intrusion Meeting*, Ghent, Belgium, pp. 132–142.

Leatherman, S. P.: 1984, Coastal Geomorphic Responses to Sea Level Rise: Galveston Bay, Texas, In: M. C. Barth and J. G. Titus, (eds), *Greenhouse Effect and Sea Level Rise: A Challenge for this Generation*, Van Nostrand Reinhold Co, New York, pp. 151–178.

Lebbe, L. C.: 1983, Mathematical model of the evolution of the fresh-water lens under the dunes and beach with semi-diurnal tides, *Proc. 8th Salt Water Intrusion Meeting*, Bari, Italy, pp. 211–226.

Lennon, G. P., Wisniewski, G. M. and Yoshioka, G. A.: 1986, Impact of increased river salinity on New Jersey aquifers, In: C. H. J. Hull and J. G. Titus (eds), *Greenhouse Effect, Sea Level Rise, and Salinity in the Delaware Estuary*, U.S. Environ. Protect. Agency and Delaware River Basin Commission, Washington DC, pp. 40–54.

McDonald, M. G. and Harbaugh, A. W.: 1988, A modular three-dimensional finite-difference ground-water flow model, U.S. Geol. Surv. Techn. of Water-Resour. Invest., Book 6, Chapter A1, 586 pp.

Meisler, H., Leahy, P. P. and Knobel, L. L.: 1984, Effect of eustatic sea-level changes on saltwater-freshwater in the northern Atlantic coastal plain, U.S. Geol. Surv. Water-Supply Paper 2255.

Navoy, A. S.: 1991, *Aquifer-estuary interaction and vulnerability of groundwater supplies to sea level rise-driven saltwater intrusion*, PhD Thesis, Pennsylvania State Univ., U.S.A., 225 pp.

Oude Essink, G. H. P.: 1996, *Impact of sea level rise on groundwater flow regimes. A sensitivity analysis for The Netherlands*. PhD Thesis, Delft University of Technology, The Netherlands, 411 pp.

Oude Essink, G. H. P. and Boekelman, R. H.: 1996, Problems with large-scale modelling of salt water intrusion in 3D, *Proc. 14th Salt Water Intrusion Meeting*, Malmö, Sweden, pp. 16–31.

Oude Essink, G. H. P.: 1998, MOC3D adapted to simulate 3D density-dependent groundwater flow, *Proc. MODFLOW'98 Conf.*, Golden, Colorado, USA, pp. 291–303.

Oude Essink, G. H. P.: 1999, Impact of sea level rise in The Netherlands, Seawater intrusion in coastal aquifers, In: J. Bear and A.H-D. Cheng *et al.* (eds), Concepts, Methods and Practices, Kluwer Academic Publishers, pp. 507–530.

Paap, H. A.: 1992, *The influence of the rise of sea level on the salinisation process. The code of Konikow-Bredehoeft applied on a 2D cross-section in Noord-Holland, The Netherlands*, (in Dutch). MSc Thesis, Delft University of Technology, The Netherlands, 139 pp.

Sanford, W. E. and Konikow, L. F.: 1985, A two-constituent solute-transport model for ground water having variable density U.S. Geol. Surv. Water-Resour. Invest., Report 85-4279, 88 pp.

Stuyfzand, P. J.: 1993, *Hydrochemistry and hydrology of the coastal dune area of the Western Netherlands*. PhD Thesis, Vrije Universiteit Amsterdam, The Netherlands, 366 pp.

TNO Institute of Applied Geoscience, Delft: 1979, In: R. Lageman and M. Homan (eds), *Ground-water Map of The Netherlands*: Alkmaar and Medemblik, (in Dutch), 70 pp.

TNO-GG/RIZA: 1994, NAGROM: report 8, supra-regio Holland-Noord, OS 94-44 TNO-GG Institute of Applied Geoscience and Rijkswaterstaat-RIZA.

Van Dam, J. C.: 1976, Partial depletion of saline groundwater by seepage, *J. Hydrol.* **29**, 315–339.

Verruijt, A.: 1980, The rotation of a vertical interface in a porous medium, *Water Resour. Res.* **16**, 239–240.

Warrick, R. A., Oerlemans, J., Woodworth, P. L., Meier, M. F. and le Provost, C.: 1996, Changes in sea level, In: J. T. Houghton, L. G. Meira Filho and B. A. Callander (eds), *Climate Change 1995: The Science of Climate*, Contribution of Working Group I to the Second Assessment Report of the Intergovernmental Panel of Climate Change, Cambridge University Press, Cambridge, pp. 359–405.

Wesseling, J.: 1980, Saline seepage in The Netherlands, occurrence and magnitude, *Research on possible changes in the distribution of saline seepage in The Netherlands*, Committee for Hydrological Research (CHO-TNO), Proc. and Informations, 26, pp. 17–33.